Journal of Biotechnology 199 (2015) 90–97

Contents lists available at ScienceDirect

Journal of Biotechnology

journal homepage: www.elsevier.com/locate/jbiotec

Effect of linker flexibility and length on the functionality of a cytotoxic engineered antibody fragment

Maximilian Klement[a,b,1], Chengcheng Liu[a,1], Bernard Liat Wen Loo[a], Andre Boon-Hwa Choo[a], Dave Siak-Wei Ow[a,**], Dong-Yup Lee[a,b,*]

[a] Bioprocessing Technology Institute, A*STAR (Agency for Science, Technology and Research), 20 Biopolis Way, #06-01 Centros, Singapore 138668, Singapore
[b] Department of Chemical and Biomolecular Engineering, Synthetic Biology Research Consortium, National University of Singapore, 4 Engineering Drive 4, Singapore 117585, Singapore

ARTICLE INFO

Article history:
Received 10 September 2014
Received in revised form 9 January 2015
Accepted 2 February 2015
Available online 16 February 2015

Keywords:
Peptide linkers
Synthetic protein engineering
Engineered antibody fragments
Recombinant fusion proteins
Molecular dynamics simulation

ABSTRACT

Engineered antibody fragments often contain natural or synthetic linkers joining the antigen-binding domain and multimerization regions, and the roles of these linkers have largely been overlooked. To investigate linker effects on structural properties and functionality, six bivalent cytotoxic antibody fragments with of linkers of varying flexibility and length were constructed: (1) 10-AA mouse IgG3 upper hinge region, (2) 20-AA mouse IgG3 upper hinge region repeat, (3) 10-AA glycine and serine linker, (4) 20-AA glycine and serine linker repeat, (5) 21-AA artificial linker, and (6) no-linker control. Interestingly, a higher cytotoxicity was observed for fragments bearing the rigid short linkers compared to the flexible longer linkers. More importantly, amino acid composition related to the rigidity/flexibility was found to be of greater importance upon cytotoxicity than linker length alone. To further study the structure–function relationship, molecular modelling and dynamics simulation were exploited. Resultantly, the rigid mouse IgG3 upper hinge region was predicted to enhance structural stability of the protein during the equilibrium state, indicating the improved cytotoxicity over other combinations of fragments. This prediction was validated by measuring the thermal stability of the mouse IgG3 upper hinge as compared to the artificial linker, and shown to have a higher melting temperature which coincides with a higher structural stability. Our findings clearly suggest that appropriate linker design is required for enhancing the structural stability and functionality of engineered antibody fragments.

1. Introduction

Engineered antibody fragments are an emerging class of recombinant fusion proteins that have thus far shown great potential as important biopharmaceuticals due to their smaller sizes relative to whole antibodies (Hu et al., 1996; Rheinnecker et al., 1996; Pluckthun and Pack, 1997; Muller et al., 1998; Shahied et al., 2004; Beckman et al., 2007; Schaefer et al., 2010). Antibody fragments can be engineered as dimers, trimers and in some cases, tetramers, mainly consisting of single-chain antibodies (scFvs), a multimerization scaffold domains, for example, dimeric GCN4 leucine zipper (ZIP) (Pack and Pluckthun, 1992) and dimeric Helix1-turn-Helix2 (Lim et al., 2011), and a peptide linker. Among the three regions that constitute the fragments, linkers play an indispensable role in joining domains (Wriggers et al., 2005; Chen et al., 2013; Reddy Chichili et al., 2013; Yu et al., 2015). Nonetheless, their functional role and significance have largely been overlooked.

In general, fusion proteins lacking suitable linkers may misfold and express at low levels (Chen et al., 2013). The linker design can be guided by the existing peptide linkers in multi-domain proteins, with an average length ranging from 4.5 (±0.7) residues to 21 (±7.6) residues (George and Heringa, 2002). Recently, it was reported that a 2–3 fold increase in length of the (G4S) linker repeat led to the improved binding affinity of a Fynomer-Fc fusion protein (Silacci et al., 2014). This indicates that linker length is one of the important parameters in the design of fusion proteins. In addition to linker length, the amino acid composition of the linker may affect the folding or expression of fusion proteins since the linker composition is related to its flexibility. Hence, it is important to investigate the effects of relevant linker design parameters on the functionality of antibody fragments.

* Corresponding author at: Department of Chemical and Biomolecular Engineering, Synthetic Biology Research Consortium, National University of Singapore, 4 Engineering Drive 4, Singapore 117585, Singapore. Tel.: +65 6516 6907; fax: +65 6779 1936.
** Corresponding author. Tel.: +65 64070843; fax: +65 6478 9561.
E-mail addresses: dave_ow@bti.a-star.edu.sg (D.S.-W. Ow), cheld@nus.edu.sg (D.-Y. Lee).
[1] These authors contributed equally to this work.

http://dx.doi.org/10.1016/j.jbiotec.2015.02.008
0168-1656/

In this study, we measured the effects of linkers on the cytotoxicity of engineered antibody fragments derived from the cytotoxic monoclonal antibody 84 (mAb84), an IgM molecule which specifically targets and kills undifferentiated human ES cells (hESCs) (Choo et al., 2008). mAb84 has applications in cell therapy, to remove residual undifferentiated hESC prior to transplant, to ensure patient safety. However, the large size of an IgM molecule (960 kDa) restricts the antibody's ability to penetrate tissues, and hence target cell clusters, therefore not eliminating all residual undifferentiated hESC from the tissue (Lim et al., 2011). Thus, we generated smaller bivalent antibody constructs where the single-chain variable fragment (scFv) of mAb84 was connected to GCN4 ZIP domain using five different linkers as well as a control with no linker. The difference in linker length and amino acid composition allowed us to hypothesize and deduce that these linkers have varied effects on the cytotoxicity towards hESCs. Homology modelling and molecular dynamic (MD) simulation were also performed to derive the 3D structures and explore the underlying physical differences of the engineered antibody fragments as related to their functionality. Furthermore, the MD simulations were validated with differential scanning calorimetry (DSC), measuring the melting temperature of the engineered antibody fragments. DSC was used to study the melting temperature of the mouse IgG3 upper hinge and the LFL linker, which showed a higher melting temperature for the mouse IgG3 upper hinge, indicating its higher structural stability.

2. Methods and materials

2.1. Plasmid construction

We used a previously engineered antibody fragment pET-scFv84-HTH (Q6E) (Lim et al., 2011) as the template, and made changes to the plasmid on the C-terminus side. The mouse IgG3 upper hinge (mIgG3UH) and ZIP domain were obtained from a synthetic gene, which was codon optimized for expression in *Escherichia coli*, and isolated by restriction enzyme digestion and purification of the gene of interest. The template and purified insert were digested with restriction enzymes, *Avr*II and *Not*I, and ligated into the pET vector. The vector, pET-scFv84-mIgG3UH-ZIP, was confirmed by DNA sequencing. Vectors for the remaining five engineered antibody fragments: scFv84-ZIP, scFv84-$(G4S)_2$-ZIP, scFv84-$(G4S)_4$-ZIP, scFv84-$(mIgG3UH)_2$-ZIP, and scFv84-LFL-ZIP, were similarly assembled from the pET-scFv84-mIgG3UH-ZIP vector and synthetic genes, codon optimized for expression in *E. coli*, comprising the linker and ZIP domains using restriction enzymes, *AvrII* and *NotI*. The vectors were confirmed by DNA sequencing. The vectors code for a monovalent component of the engineered antibody fragments, with each plasmid coding for the signal peptide (pelB), scFv84 (including mAb84 heavy chain variable domain, $(G4S)_3$ linker, and mAb84 light chain variable domain), linker, ZIP domain, spacer and His-tag.

2.2. Expression, isolation, and purification

The DNA constructs were transformed into *E. coli* cells BL21 (DE3) and selected on kanamycin (30 μg/mL)-containing Luria-Bertani (LB) agar plates. Overnight culture of *E. coli* carrying the three vectors were grown in 2xYT medium (16 g/L tryptone, 10 g/L yeast extract, 5 g/L NaCl) containing kanamycin (30 μg/mL) and 1 g/L glucose for about 2 h at 37 °C until an optical density at 600 nm (OD600) of 0.6–0.8 was reached. Expression was induced with isopropyl β-D-1-thiogalactopyranoside (IPTG) at a final concentration of 0.1 mM, and the culture incubated at 30 °C thereafter. The cells were harvested 5 h post-induction by centrifugation.

The cell pellets underwent periplasmic extraction by osmotic shock, with the protein separated by centrifugation at 17,000 × *g* for 1 h as described (Lim et al., 2011). The supernatant was concentrated and buffer exchanged with a Vivaflow 200, 10 k molecular weight cut-off Hydrosart membrane (Sartorius, Goettingen, Germany) to 100 mL of the volume in phosphate-buffered saline (PBS), pH 7.4. The sample was applied to a 1 mL HiTrap FF pre-charged with Co^{2+}, to allow the His-tagged engineered antibody fragments to bind. The fragments were washed with 5 column volumes of PBS buffer (pH 7.4) containing imidazole at 10 mM and eluted in the same buffer with 400 mM imidazole. Eluted engineered antibody fragments were concentrated by using Vivaspin (10-kDa molecular mass cutoff) spin concentrators (Sartorius Stedim, Goettingen, Germany). Protein concentrations were determined using the Nanodrop spectrophotometer (Thermo Scientific). The proteins were separated on 4–12% Bis–Tris gels (NuPAGE® Novex Bis Tris gels, NuPAGE® System, Invitrogen) and visualized with Coomassie Brilliant Blue (Thermo Scientific, Rockford, IL).

2.3. Analytical size-exclusion chromatography

The engineered antibody fragments were analyzed on a Shimadzu HPLC system (Shimadzu, Columbia, MD, USA) with a Dual Wavelength Detector. A Superdex75 PC 3.2/30 size-exclusion chromatography (SEC) column (GE Healthcare, Uppsala, Sweden) was equilibrated with 200 mM arginine, 50 mM bicine, 5 mM EDTA, 0.005% sodium azide, pH 8.0. Protein samples between 0.25 and 0.5 mg/mL were filtered through a 0.22 μm filter before loading into the instrument. The chromatogram was analyzed using the vendor's software (Shimadzu, Columbia, MD, USA) to calculate the peak values and retention time.

2.4. Fluorescence activated cell sorting

Binding and cytotoxicity of the engineered antibody fragments were evaluated on the hESC line, HES-3 (ESI, Singapore). Single-cell suspensions of hESC were harvested using trypsin and resuspended in 1% BSA/1× PBS. For experiments with live hESC staining, 100 μL (estimated 1×10^5 cells) of hESC were incubated separately with each engineered antibody fragment at 4 °C for 30 min. Cells were washed and resuspended in 1% BSA/PBS. Purified engineered antibody fragments were buffer exchanged with phosphate-buffered saline (PBS) with 10 mM imidazole and conjugated to a penta·His Alexa Fluor 647. Binding of engineered antibody fragments to cells was monitored using flow cytometry (BD FACS Calibur, BD Biosciences, San Jose, CA, USA). Cytotoxicity was determined by propidium iodide (1.25 mg/mL) exclusion using flow cytometry and normalized with respect to the buffer control (Tan et al., 2009).

2.5. Homology modelling

A monovalent engineered antibody fragment in this study consisted of a single-chain variable fragment (scFv84), a leucine zipper (ZIP) and a linker joining the two domains together. Five linkers were used: $(G4S)_2$, $(G4S)_4$, mIgG3UH, $(mIgG3UH)_2$ and the long flexible linker (LFL) used by Cuesta and colleagues (2009). Structural models of six monovalent engineered antibody fragments were built: scFv84-ZIP, scFv84-$(G4S)_2$-ZIP, scFv84-$(G4S)_4$-ZIP, scFv84-mIgG3UH-ZIP, scFv84-$(mIgG3UH)_2$-ZIP and scFv84-LFL-ZIP. These models were subsequently used to build the bivalent form of engineered antibody fragments for illustration.

The structure of the scFv84 was modelled by homology modelling software MODELLER in Discovery Studio 2.5 using Protein Data Bank (PDB) structure 2GHW_B, 1QOK_A, 4CAU_D, 1SM3_H, 1DZB_A, 3GKZ_A, 3UYP_A, 3NZH_H, 4GQP_H, 2GKI_A, 1PZ5_B,

1M71_B, 1SBS_H, 1NQB_A and 1F3R_B as the templates, which were identified with a blast *e*-value of less than 2.8*e*−60. The structure of ZIP was built using [PDB:3BAS_A] as the template with a blast e-value of 7.5*e*−12 (Accelrys Software Inc.). Twenty-five models were built for both scFv84 and ZIP domains. The best homology model of each domain was chosen based on the Probability Density Function (PDF) total energy calculated by MODELLER. Profiles-3D and Ramachandran plot statistics were then used to verify the best homology models (Table 2). The obtained homology models of scFv84 and ZIP were joined together to form the monovalent engineered antibody fragment of scFv84-ZIP. To form the monovalent engineered antibody fragments containing linkers, the connection was done by adding the N-terminal end of the linker after residue A239 at the C-terminal end of the scFv84 domain, and adding the C-terminal end of the linker before residue R1 at the N-terminal end of the ZIP domain. In the simulation, the linker region was modelled to adopt the polyproline II helix ($\varphi = -78^\circ$, $\psi = 149^\circ$). The bivalent form of engineered antibody fragments were then constructed by superimposing the ZIP domain to structure [PDB:1CE9]. The angles defined between the two scFv84 centroids and N-terminal of ZIP domain in these bivalent forms were set to be about 120°. The models of bivalent engineered antibody fragments were energy minimized by a conjugate gradient procedure to remove steric hindrance or inappropriate contacts.

2.6. Molecular dynamics simulation

The generated bivalent models of scFv84-ZIP, scFv84-$(G4S)_2$-ZIP, scFv84-$(G4S)_4$-ZIP, scFv84-mIgG3UH-ZIP, scFv84-$(mIgG3UH)_2$-ZIP, scFv84-LFL-ZIP and single scFv84 were used as the initial structures for molecular dynamics simulation. Simulation experiments were conducted using GROMACS with force-field oplsa-aa (Berendsen et al., 1995; Lindahl et al., 2001; van der Spoel et al., 2005; Hess et al., 2008; Pronk et al., 2013). Each of these systems was solvated in a triclinic box. Simple point charge (SPC) model was applied to the water molecules, which were constrained to the box edges with at least 5 Å. All solvated systems were restrained with periodic boundary conditions. To remove the steric hindrance in each protein system, energy minimization was performed using the steepest descents algorithm (10,000 steps), followed by conjugate gradients algorithm (10,000 steps) with a tolerance of 20 kJ/mol/nm. Positional restraint MD simulation was then carried out for 100 ps at 300 K on the protein atoms. This was followed by a 50 ps simulated annealing procedure by heating the system from 50 K to 300 K. A final 10 ns production MD simulation was performed at 300 K to each system using isothermal coupling method with velocity rescaling. The time step was 0.002 ps. The embedded GROMACS tools were used to analyze the trajectories. Additional shell scripts and R package were applied to analyze the data.

2.7. Differential scanning calorimetry

The thermodynamic stability of the engineered antibody fragments were compared by DSC (Microcal). We found unfolding of the engineered antibody fragments to be irreversible under the conditions tested and therefore made no attempt to calculate the free energies of unfolding or any other thermodynamic parameters. Instead, the T_m values were used to determine the stability of each

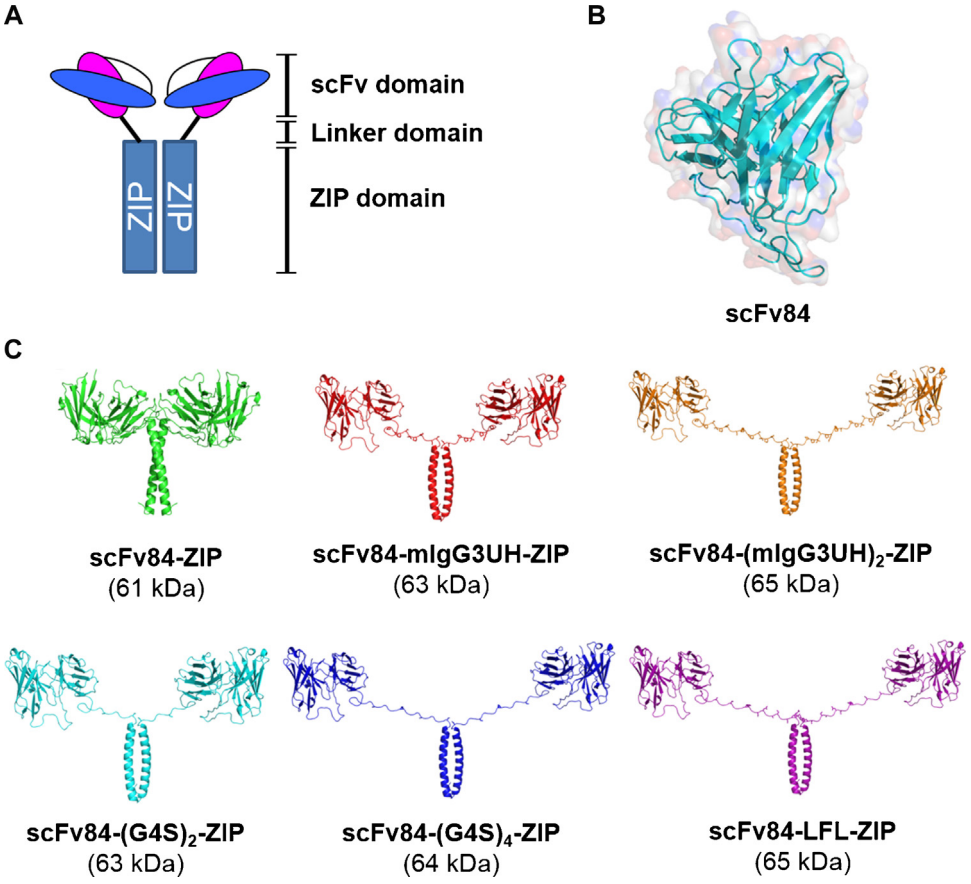

Fig. 1. Schematic overview and protein structures of the engineered antibody fragments. (A) Overview of the scFv, linker and multimerization domains in the engineered antibody fragments. Structural models were derived from homology modelling. Solid ribbon representation of the structural models of the (B) scFv84, and (C) scFv84-ZIP, scFv84-mIgG3UH-ZIP, scFv84-$(mIgG3UH)_2$-ZIP, scFv84-$(G4S)_2$-ZIP, scFv84-$(G4S)_4$-ZIP, scFv84-LFL-ZIP. scFv84: single-chain variable fragment of mAb84; mIgG3UH: mouse IgG3 upper hinge; G4S: glycine and serine composed linkers with different number of repeats; LFL: the 21-AA long flexible linker as described by Cuesta et al. (2009).

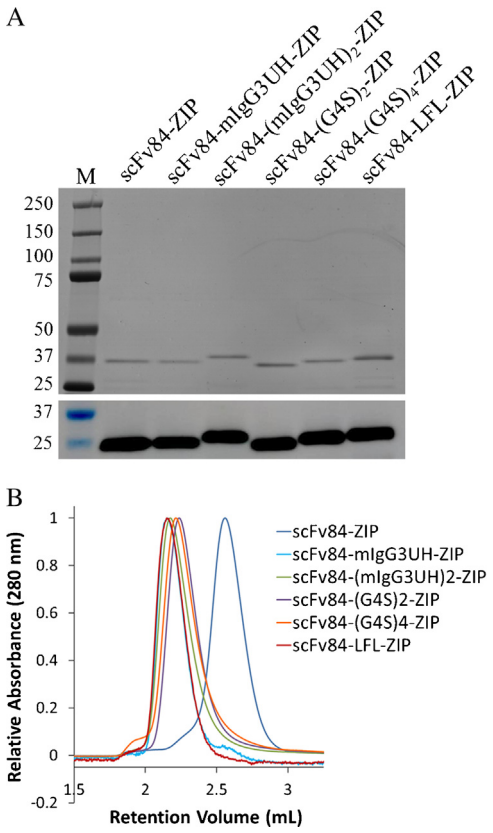

Fig. 2. Analysis of purity of engineered antibody fragments by (A) SDS-PAGE and Western blot, and (B) SEC. The monomeric engineered antibody fragments were expressed in *E. coli*, and purified after assembly into a dimeric protein using His_6 tag affinity chromatography. The purified protein was analyzed by SDS-PAGE and Western blot, and SEC.

protein as calculated by the deconvolution analysis using a non-two state model. The engineered antibody fragments were analyzed at a concentration of 0.5 mg/mL in 10 mM phosphate buffered saline (PBS) pH 7.4 buffer at a 1.0 °C/min scan rate. The proteins were analyzed by subtraction of the reference data, normalization to the protein concentration and DSC cell volume, and interpolation of a baseline. The peaks were deconvoluted by non-2-state fit.

3. Results and discussion

3.1. Engineering and expression of antibody fragments with various linkers

Engineered antibody fragments are primarily composed of three domains including a scFv antigen binding site, a multimerization region and a peptide linker (Fig. 1A). For the binding domain, we derived an antibody fragment (scFv84) from the cytotoxic parental monoclonal antibody, mAb84 (Choo et al., 2008). In turn, we used a dimeric ZIP as the multimerization domain due to its ability to bind to itself through hydrostatic interactions arranged in a 'knobs into holes' configuration. Subsequently, both domains were connected by a linker, carefully selected by considering its characteristics: the linker can affect the structural properties and functionality of the bivalent engineered antibody fragments although it does not interfere with the native folding of each domain.

First, two types of common linkers, the mIgG3UH (rigid) and the (G4S) repeat (flexible), and a synthetic linker (flexible) were used to emulate a variety of combinational characteristics, from short and rigid to long and flexible. The mIgG3UH and $(mIgG3UH)_2$ are 10-AA and 20-AA long, respectively, with a high percentage of proline (40%). It should be noted that proline-rich linkers are

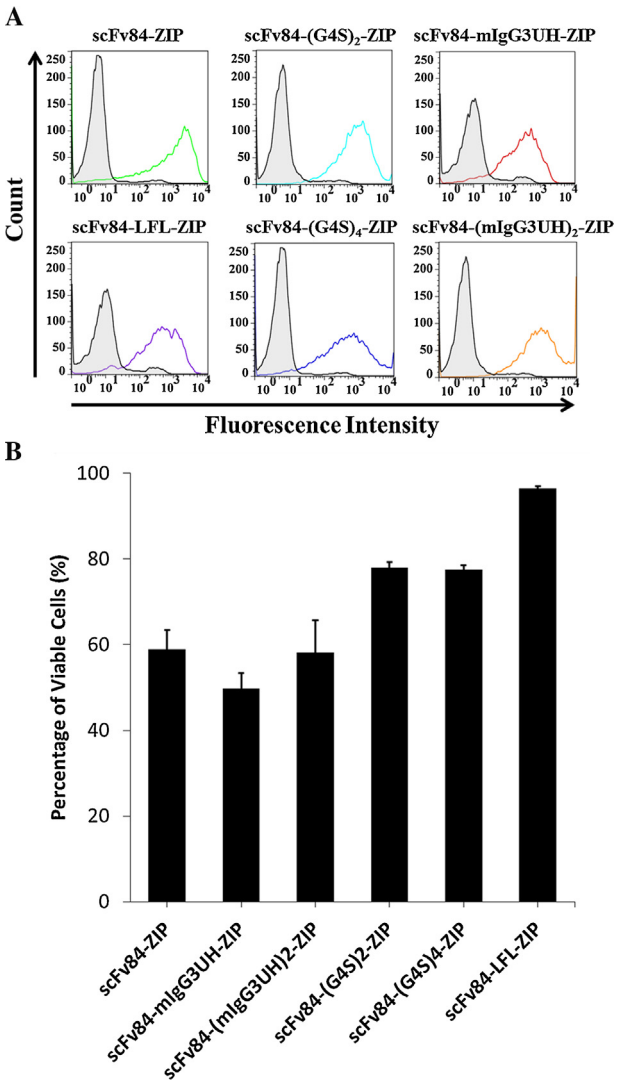

Fig. 3. Analysis of binding and cytotoxicity of the engineered antibody fragments to undifferentiated human embryonic stem cells line, HES-3, by flow cytometry. Cells were incubated with 100 μg of the engineered antibody fragments at 4 °C for 30 min, after which cells were harvested for analysis by propidium iodide exclusion assay on the flow cytometer ($n = 3$). (A) The engineered antibody fragments (scFv84-ZIP, green; scFv84-mIgG3UH-ZIP, red; scFv84-$(mIgG3UH)_2$-ZIP, orange; scFv84-$(G4S)_2$-ZIP, light blue; scFv84-$(G4S)_4$-ZIP, blue; scFv84-LFL-ZIP, purple) bound to HES-3 cells were detected with Alexa Fluorophore 647 conjugated anti-His antibody. The shaded histogram represents the negative control. (B) The cytotoxicity of the engineered antibody fragments were analyzed using a propidium iodide exclusion assay, and reported as the percentage of viable cells. All error bars represent ± SEM. (For interpretation of the references to colour in this figure legend, the reader is referred to the web version of this article.)

relatively rigid and thus have an increased stability and biological activity in recombinant fusion proteins (Zhao et al., 2008; Haga et al., 2013). In contrast, the $(G4S)_2$, $(G4S)_4$, and LFL artificial linker are rich in glycines. These linkers may grant the bivalent engineered antibody fragments a higher rotational freedom, hence higher flexibility. In all, we generated five variations of linkers with respect to the amino acid composition (proline-rich versus glycine-rich) and length, scFv84-$(G4S)_2$-ZIP, scFv84-mIgG3UH-ZIP, scFv84-$(G4S)_4$-ZIP, scFv84-$(mIgG3UH)_2$-ZIP, and scFv84-LFL-ZIP (Table 1). In addition, a sixth engineered antibody fragment with no linker, scFv84-ZIP, was introduced as the control. Based on the variations in linker, we constructed six engineered antibody fragments, the structures of which were visualized using homology models (Fig. 1C).

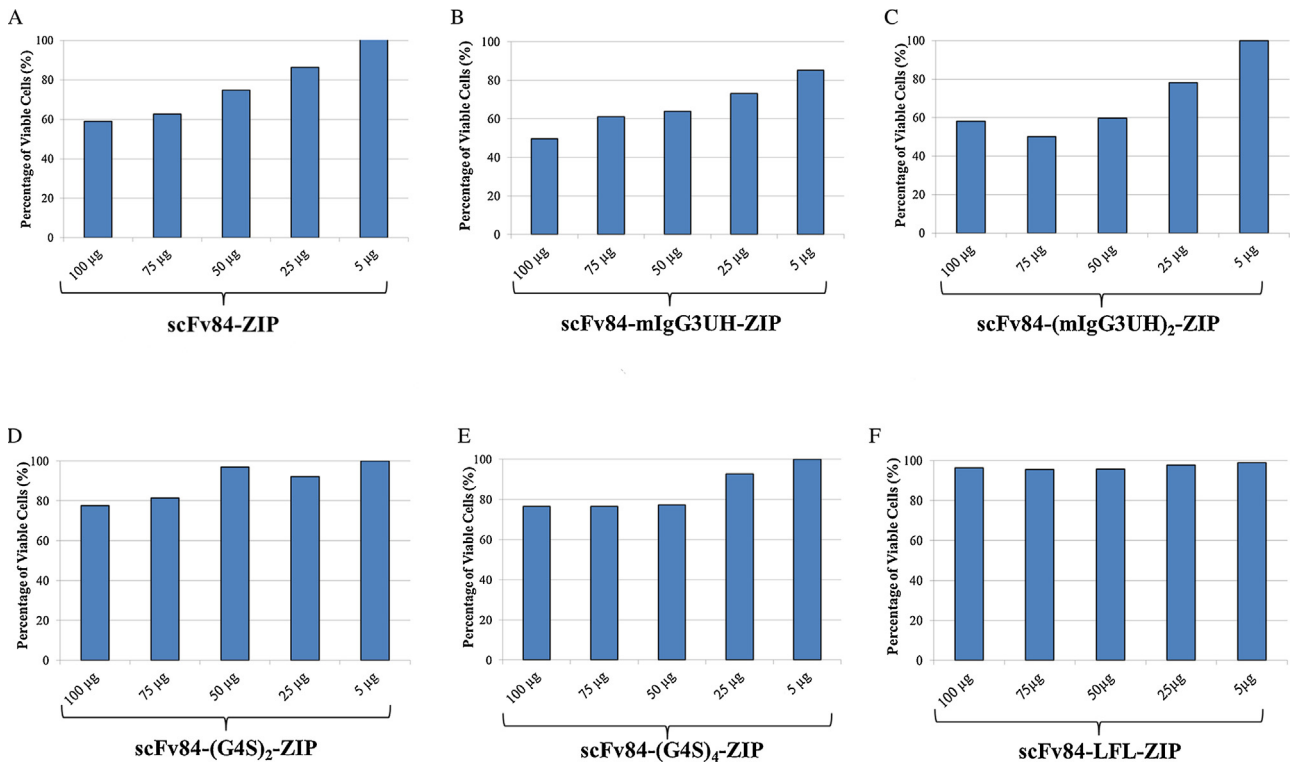

Fig. 4. Dose-dependent cytotoxicity of the engineered antibody fragments. hESC were incubated with 100 µg, 75 µg, 50 µg, 25 µg, and 5 µg of the engineered antibody fragments at 4 °C for 30 min, after which cells were harvested for analysis by propidium iodide exclusion assay on the flow cytometer. The cytotoxicity at each dose was studied for (A) scFv84-ZIP, (B) scFv84-mIgG3UH-ZIP, (C) scFv84-(mIgG3UH)$_2$-ZIP, (D) scFv84-(G4S)$_2$-ZIP, (E) scFv84-(G4S)$_4$-ZIP, and (F) scFv84-LFL-ZIP.

The engineered antibody fragments were expressed in *E. coli* BL21 (DE3) and purified by buffer exchange, affinity chromatography, and ultrafiltration using a 10 kDa molecular weight cut-off membrane. All fragments were secreted to the periplasm at approximately the same yield. After purification, SDS-PAGE and Western blot (Fig. 2A) and size exclusion chromatography (SEC) (Fig. 2B) were performed to evaluate protein purity. SDS-PAGE analysis of the denatured proteins showed a singular protein band of high purity with the expected molecular weight of the monomeric fragments. Western blot analysis confirmed the protein band to correspond to the appropriate engineered antibody fragment. All engineered antibody fragments were estimated to have a purity of at least 90%. The samples were further analyzed by SEC, resulting in a peak between a retention volume of 1.5 mL and 3 mL, which coincides with the expected elution volume for the molecular weight (approximately 64 kDa) of the dimeric antibody fragments. All engineered antibody fragments have similar molecular weights, except for scFv84-ZIP, due to the absence of a linker it has a lower molecular weight, thus, elutes later in the chromatogram. The SEC analysis confirmed the assembly of the monomeric constructs into the bivalent antibody fragments.

3.2. Effect of linkers in engineered antibody fragments on cytotoxicity

In order to explore the cytotoxic effect of linkers, the binding of the engineered antibody fragments to hESC was measured by a penta·His Alexa fluor 647 conjugate and analyzed with fluorescence activated cell sorting. This functional activity of the fragments towards the target, HES-3 cells, are confirmed by an increase in fluorescence intensity (a shift to the right) in comparison to the negative control (shaded area) (Fig. 3A). Furthermore, an overlay of the histograms with each other as well as with scFv84 (Lim et al., 2011) proved similar binding profiles, while the buffer control had no binding or cytotoxicity (results not included). Thus, we can deduce that the antigen-binding mechanism was not altered by engineering the antibody fragments. However, this gave a rise to a change in their functionality over a two fold range (Fig. 3B).

Functional activity of the engineered antibody fragments was quantified using a cytotoxic live/dead stain based on propidium iodide exclusion. Cytotoxicity of mAb84 was a result of binding to PODXL-1, a highly glycosylated sialomucin, on the cell-surface (Choo et al., 2008). Upon binding to the cell-surface receptor,

Table 1
Designations and linkers used for the engineered antibody fragments.

Designation	Single-chain antibody fragment (scFv) [C-terminus]	Linker	GCN4 leucine zipper (ZIP) [N-terminus]
scFv84-ZIP	scFv84-	–	-RMKQLEDKVEELLSKNYHLENEVARLKKLVGER
scFv84-mIgG3UH-ZIP	scFv84-	-PKPSTPPGSS-	-RMKQLEDKVEELLSKNYHLENEVARLKKLVGER
scFv84-(mIgG3UH)$_2$-ZIP	scFv84-	-PKPSTPPGSSPKPSTPPGSS-	-RMKQLEDKVEELLSKNYHLENEVARLKKLVGER
scFv84-(G4S)$_2$-ZIP	scFv84-	-GGGGSGGGGS-	-RMKQLEDKVEELLSKNYHLENEVARLKKLVGER
scFv84-(G4S)$_4$-ZIP	scFv84-	-GGGGSGGGGSGGGGSGGGGS-	-RMKQLEDKVEELLSKNYHLENEVARLKKLVGER
scFv84-LFL-ZIP	scFv84-	-NSGAGGSGGSSGSDGASGSRD-	-RMKQLEDKVEELLSKNYHLENEVARLKKLVGER

The designations of the engineered antibody fragments used in this work are given. All constructs are based on a C-terminal single-chain variable fragment of monoclonal antibody 84 (scFv84) (Choo et al., 2008) and a N-terminal GCN4 leucine zipper (ZIP) domain with a linker region. A no linker control, scFv84-ZIP, is included. The five peptide linkers used are: mouse IgG3 upper hinge (mIgG3UH), scFv84-(mIgG3UH)$_2$-ZIP, scFv84-(G4S)$_2$-ZIP, scFv84-(G4S)$_4$-ZIP, and the 21-AA long flexible linker (LFL) as described by Cuesta et al. (2009).

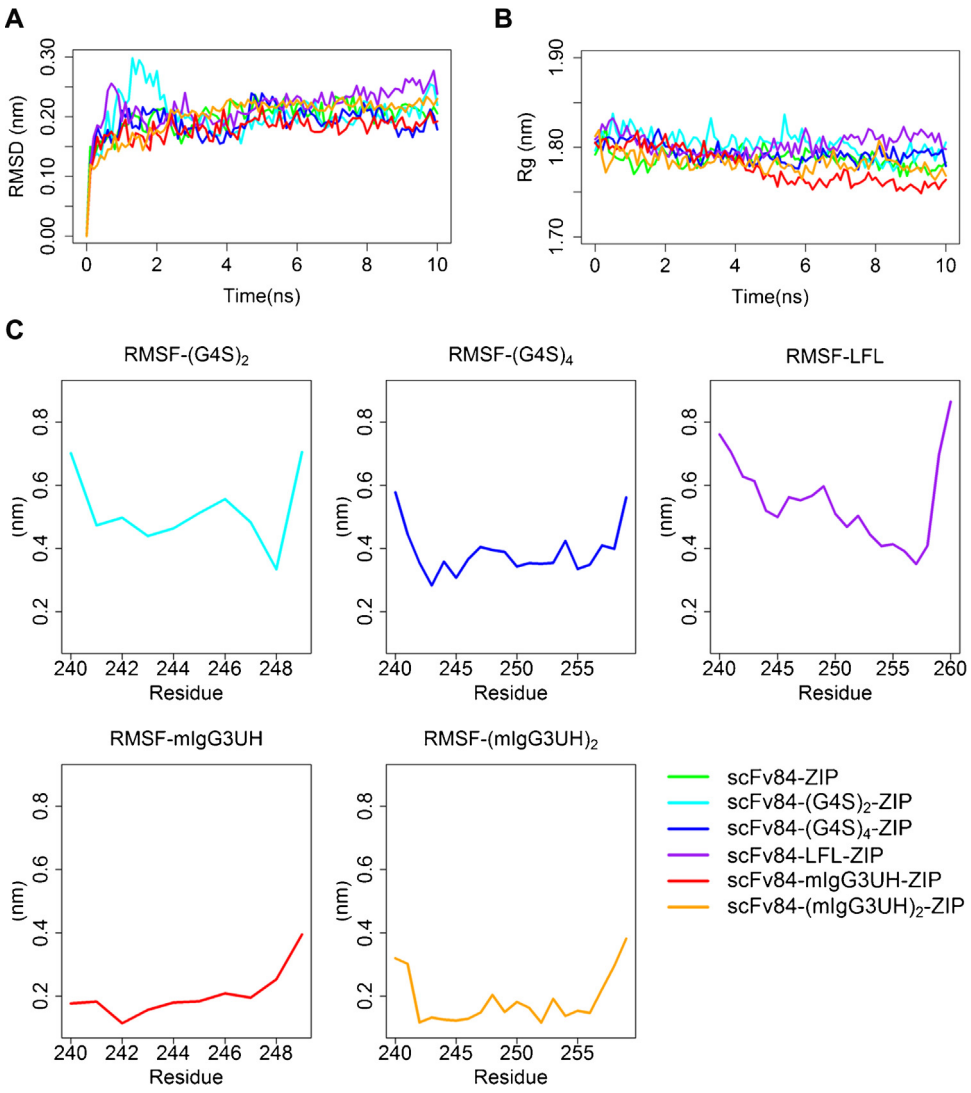

Fig. 5. Molecular dynamics simulation of engineered antibody fragments. (A) RMSD of the backbone atoms of the monomer, (B) radius of gyration of the dimer, (C) RMSF of the linker region. scFv84-ZIP (green); scFv84-mIgG3UH-ZIP (red); scFv84-$(mIgG3UH)_2$-ZIP (orange); scFv84-$(G4S)_2$-ZIP (light blue); scFv84-$(G4S)_4$-ZIP (blue); scFv84-LFL-ZIP (purple). (For interpretation of the references to colour in this figure legend, the reader is referred to the web version of this article.)

degradation and rearrangement of the actin-associated proteins α-actinin, paxillin and tallin enable the aggregation of PODXL-1 by mAb84, resulting in the formation of pores in the cell membrane as seen by scanning electron microscopy. The formation of pores leads to the leakage of intracellular Na^+, a process termed oncosis (Tan et al., 2009). Oncosis is characterized by rapid cell death as a result of chemical toxicity as induced by mAb84 in this case, which lies in contrast to apoptosis, programmed cell death. The engineered scFv84 antibody fragments are expected to undergo the same biological killing process due to the unmodified binding site isolated from mAb84.

We observed that an optimal protein amount of 100 μg produced the highest functional disparity, thus suggesting that the cytotoxic distribution is attributable to the saturated binding of cells with the engineered antibody fragments. Therefore, the structure becomes the principal characteristic in the functional study. At lower protein amounts, the disparity between the antibody fragments is less significant (Fig. 4). As the dosage is reduced, the cytotoxicity decreases linearly for all fragments. Thus, the relationship between cytotoxicity and the engineered antibody fragments is dose-dependent. The resultant cytotoxicity assay in Fig. 3B allowed us to quantitatively analyze the functional role of the linkers within the engineered antibody fragments, as all other domains were held equal. In comparison to scFv84-ZIP, the short mIgG3UH linker improved the functionality, whereas the G4S and LFL linkers had a reduced effect. The short mIgG3UH linker had a 10% increased cytotoxicity compared to the no linker control. However, this was negated when the length of the mIgG3UH linker increased 2 fold. On the other hand, the G4S linkers had a 20% decrease in functional impact with respect to the no linker control, with the increase in length having little effect upon the HES cells. Similarly, the LFL linker had little impact upon cell viability, with approximately 90% of the cells being live after treatment, in comparison only 60% of the HES cells were viable after treatment with the no linker control.

Based on our experimental observation, we inferred that amino acid composition is a more relevant design parameter for linker selection for engineering antibody fragments than linker length. However, the current analysis results do not enable further conclusions to be drawn to understand the molecular impact of linker flexibility upon cytotoxicity. Thus, molecular dynamics (MD) simulations were used to provide high-resolution spatial and temporal data on the folding and stability of the fusion protein.

Table 2
Ramachandran statistics for the homology models of antibody fragments.

Structure model	Ramachandran statistics (%)		
	Allowed regions	Marginal regions	Disallowed regions
scFv84	95.4	2.6	2.0
scFv84-ZIP	96.1	2.2	1.8
scFv84-mIgG3UH-ZIP	95.7	2.6	1.7
scFv84-$(mIgG3UH)_2$-ZIP	95.4	2.9	1.7
scFv84-$(G4S)_2$-ZIP	95.7	2.6	1.7
scFv84-$(G4S)_4$-ZIP	95.3	3.0	1.7
scFv84-LFL-ZIP	94.6	3.3	2.1

The values indicate the percentages of residues that are grouped into the allowed, marginal and disallowed regions in the Ramachandran plot.

3.3. Molecular dynamic simulations and differential scanning calorimetry analysis of the engineered antibody fragments

MD simulations have emerged as an indispensable tool in the analysis of complex molecular systems, obtaining an informative view of structure and dynamics. In order to run the simulations, we can consider homology models as a backbone or template since no crystal structure of our systems has been solved so far. Thus, we built homology models to construct the 3D structures of free scFv84 (Fig. 1B; Table 2) and bivalent engineered antibody fragments, which consisted of scFv84, ZIP domain and the linker (Fig. 1C). The average structural properties of scFv84 in the bivalent models were assessed from the trajectory files.

Prior to analysing the structural properties of the bivalent engineered antibody fragments, the quality of the MD simulation was checked by backbone root mean squared deviation (RMSD) where an equilibration state should be reached (Fig. 5A). The curves of scFv84-ZIP, scFv84-mIgG3UH-ZIP and scFv84-$(mIgG3UH)_2$-ZIP stabilized over a shorter time duration as compared to scFv84-$(G4S)_2$-ZIP, scFv84-$(G4S)_4$-ZIP and scFv84-LFL-ZIP. Subsequently, the average radius of gyration of the two scFv84s in the fragments was calculated in Fig. 5B and found to oscillate between 1.75 nm and 1.85 nm. Hence, it gives a measure of the shape of the molecule at each time point. It is noteworthy to observe that the radius of scFv84 in scFv84-mIgG3UH-ZIP has a decreasing trend, indicating that the antibody domain becomes more folded and stable.

Further analysis of the engineered antibody fragment was performed by the root mean square fluctuation (RMSF), capturing the fluctuation of each atom within the linker about its average position (Fig. 5C). This gives insight into the flexibility of the linker regions in the fragments. The GS linkers are more flexible with RMSF values ranging above 0.3 nm for each residue; while, the Pro-rich linkers have RMSF values ranging from 0.15 to 0.4 nm. Furthermore, proline-rich linkers (mouse IgG3 linker) have smaller fluctuations at its N-terminal end compared to glycine-rich linkers (G4S and the artificial linker). Thus, we can propose that the amino acid composition of the linker affect the stability and folding of scFv84 in the bivalent systems with proline-rich linkers, thereby enhancing the cytotoxicity. Such influence is independent of the linker length. On the other hand, the G4S linkers increase the flexibility of the entire bivalent system (Fig. 5C); hence they can lead to too much flexibility and thus disrupt the stability of the bivalent systems as observed in the RMSD plots (Fig. 5A). As MD simulations proposed that the longer and flexible (G4S)4-ZIP linkers reduced the protein stability of the scFv domain, the thermal melting temperature of each fragment as determined by calorimetry was measured. Characteristically, scFv and leucine zipper each produce separate peaks corresponding to the melting temperatures as each protein unfolds. T_{m2} and T_{m3} correspond to VL and VH of the scFv domain, while T_{m4} corresponds to the leucine zipper. A higher melting temperature coincides with higher protein stability, whereas a lower melting temperature corresponds to lower protein stability. From Table 3, it can be seen that the scFv84-(G4S)4-ZIP showed the lowest T_{m2} and T_{m3} (53.13 and 57.50 respectively) over other engineered antibody fragments.

Table 3
Protein stability of the engineered antibody fragments as determined by differential scanning calorimetry.

Engineered antibody fragment	Melting temperature (°C)			
	T_{m1}	T_{m2}	T_{m3}	T_{m4}
scFv84		57.38	59.98	
scFv84-ZIP	51.54	57.13	60.39	69.32
scFv84-mIgG3UH-ZIP	51.22	56.99	60.66	69.37
scFv84-$(mIgG3UH)_2$-ZIP	52.32	56.83	60.61	69.11
scFv84-$(G4S)_2$-ZIP		57.09	61.03	69.13
scFv84-$(G4S)_4$-ZIP		53.13	57.50	68.52
scFv84-LFL-ZIP		56.62	60.92	69.01

The values indicate the melting temperatures of each peak as determined by the deconvolution analysis of the chromatograms (Supp. Fig. S1). An unmodified scFv fragment was run as a control with two peaks at approximately 57.38 °C and 59.98 °C, which coincided with the melting temperatures of the VL and VH (T_{m2} and T_{m3} in Table 3). In addition, based on previously published results, the dimeric GCN4 leucine zipper has a melting temperature at approximately 70 °C. This coincided with the melting temperature of the fourth peak (T_{m4}) in the chromatogram.

4. Conclusions

In this study, we investigated the effect of flexibility and length of linkers in engineered antibody fragments on their functional activity. The linker region provides rotational freedom to the bivalent engineered antibody fragments; however, its role in impacting the structure and functionality has not been fully explored. We used a no linker control, a mouse IgG3 upper hinge region linker, a glycine and serine linker, and a 21-AA artificial linker (Fig. 3B) to study their effects on the cytotoxicity of the engineered antibody fragments. While an increase in linker flexibility and length would enable the antibody binding regions to have greater flexibility to bind to the target, a rigid amino acid linker composition and a shorter linker had a greater cytotoxic impact. To understand the linker's relationship to its functionality, we built structural models, performed MD simulations, and structural stability experiments. In summary, the 10-residue mIgG3UH linker, shown to render the highest functionality, proved to be the best linker sequence because it is able to maintain its stability and simultaneously provide flexibility to the system. Therefore, the amino acid composition of the linker has a greater impact upon both flexibility and stability of the bivalent systems compared to length, to achieve the highest degree of functionality. Furthermore, we believe the next step forward is to develop an in silico tool to predict and optimize linkers based on the structural stability and functionality of recombinant fusion proteins. The outcome would lead to reduced time and cost in developing recombinant fusion proteins, which have turned into an emerging group of biopharmaceuticals.

Acknowledgements

This work was supported by the National University of Singapore, Biomedical Research Council of A*STAR (Agency for Science, Technology and Research), A*STAR Graduate Academy (A*GA), Singapore, and a grant from the Next-Generation BioGreen 21 Program (SSAC, No. PJ01109405), Rural Development Administration, Republic of Korea. We thank Dr. Victor Wong for the guidance on the cloning and protein expression work, Jeremy Lee for his help in the purification and high-performance liquid chromatography analysis of the antibody fragments, and Dr. Tan Heng-Liang for critical review of the manuscript. We also thank

Jiyun Zhang for providing hESCs and expert advice in using and analyzing the flow cytometry data.

Appendix A. Supplementary data

Supplementary data associated with this article can be found, in the online version, at http://dx.doi.org/10.1016/j.jbiotec.2015.02.008.

References

Accelrys Software Inc., 2013. Discovery Studio Modeling Environment, Release 2.5. Accelrys Software Inc., San Diego.

Beckman, R.A., Weiner, L.M., Davis, H.M., 2007. Antibody constructs in cancer therapy: protein engineering strategies to improve exposure in solid tumors. Cancer 109, 170–179.

Berendsen, H.J.C., van der Spoel, D., van Drunen, R., 1995. GROMACS: a message-passing parallel molecular dynamics implementation. Comput. Phys. Commun. 91, 43–56.

Chen, X., Zaro, J.L., Shen, W.C., 2013. Fusion protein linkers: property, design and functionality. Adv. Drug Deliv. Rev. 65 (10), 1357–1369.

Choo, A.B., Tan, H.L., Ang, S.N., Fong, W.J., Chin, A., Lo, J., Zheng, L., Hentze, H., Philp, R.J., Oh, S.K.W., Yap, M., 2008. Selection against undifferentiated human embryonic stem cells by a cytotoxic antibody recognizing podocalyxin-like protein-1. Stem Cells (Dayton, Ohio) 26, 1454–1463.

Cuesta, A.M., Sanchez-Martin, D., Sanz, L., Bonet, J., Compte, M., Kremer, L., Blanco, F.J., Oliva, B., Alvarez-Vallina, L., 2009. In vivo tumor targeting and imaging with engineered trivalent antibody fragments containing collagen-derived sequences. PLoS ONE 4, e5381.

George, R.A., Heringa, J., 2002. An analysis of protein domain linkers: their classification and role in protein folding. Protein Eng. 15, 871–879.

Haga, T., Hirakawa, H., Nagamune, T., 2013. Fine tuning of spatial arrangement of enzymes in a PCNA-mediated multienzyme complex using a rigid poly-L-proline linker. PLOS ONE 8, e75114.

Hess, B., Kutzner, C., van der Spoel, D., Lindahl, E., 2008. GROMACS 4: algorithms for highly efficient, load-balanced, and scalable molecular simulation. J. Chem. Theory Comput. 4, 435–447.

Hu, S., Shively, L., Raubitschek, A., Sherman, M., Williams, L.E., Wong, J.Y., Shively, J.E., Wu, A.M., 1996. Minibody: a novel engineered anti-carcinoembryonic antigen antibody fragment (single-chain Fv-CH3) which exhibits rapid, high-level targeting of xenografts. Cancer Res. 56, 3055–3061.

Lim, D.Y., Ng, Y.H., Lee, J., Mueller, M., Choo, A.B., Wong, V.V., 2011. Cytotoxic antibody fragments for eliminating undifferentiated human embryonic stem cells. J. Biotechnol. 153, 77–85.

Lindahl, E., Hess, B., van der Spoel, D., 2001. GROMACS 3.0: a package for molecular simulation and trajectory analysis. J. Mol. Model. 7, 306–317.

Muller, K.M., Arndt, K.M., Strittmatter, W., Pluckthun, A., 1998. The first constant domain (C(H)1 and C(L)) of an antibody used as heterodimerization domain for bispecific miniantibodies. FEBS Lett. 422, 259–264.

Pack, P., Pluckthun, A., 1992. Miniantibodies: use of amphipathic helices to produce functional, flexibly linked dimeric FV fragments with high avidity in *Escherichia coli*. Biochemistry 31, 1579–1584.

Pluckthun, A., Pack, P., 1997. New protein engineering approaches to multivalent and bispecific antibody fragments. Immunotechnology 3, 83–105.

Pronk, S., Pall, S., Schulz, R., Larsson, P., Bjelkmar, P., Apostolov, R., Shirts, M.R., Smith, J.C., Kasson, P.M., van der Spoel, D., Hess, B., Lindahl, E., 2013. GROMACS 4.5: a high-throughput and highly parallel open source molecular simulation toolkit. Bioinformatics 29, 845–854.

Reddy Chichili, V.P., Kumar, V., Sivaraman, J., 2013. Linkers in the structural biology of protein–protein interactions. Protein Sci. 22, 153–167.

Rheinnecker, M., Hardt, C., Ilag, L.L., Kufer, P., Gruber, R., Hoess, A., Lupas, A., Rottenberger, C., Pluckthun, A., Pack, P., 1996. Multivalent antibody fragments with high functional affinity for a tumor-associated carbohydrate antigen. J. Immunol. 157, 2989–2997.

Schaefer, J.V., Lindner, P., Plückthun, A., 2010. Antibody Engineering: Miniantibodies, 2nd ed. Springer Verlag, Berlin, Heidelberg, Germany.

Shahied, L.S., Tang, Y., Alpaugh, R.K., Somer, R., Greenspon, D., Weiner, L.M., 2004. Bispecific minibodies targeting HER2/neu and CD16 exhibit improved tumor lysis when placed in a divalent tumor antigen binding format. J. Biol. Chem. 279, 53907–53914.

Silacci, M., Baenziger-Tobler, N., Lembke, W., Zha, W., Batey, S., Bertschinger, J., Grabulovski, D., 2014. Linker length matters: fynomer-Fc fusion with an optimized linker displaying picomolar IL-17A inhibition potency. J. Biol. Chem. 289 (20), 14392–14398.

Tan, H.L., Fong, W.J., Lee, E.H., Yap, M., Choo, A., 2009. mAb 84, a cytotoxic antibody that kills undifferentiated human embryonic stem cells via oncosis. Stem Cells 27, 1792–1801.

van der Spoel, D., Lindahl, E., Hess, B., Groenhof, G., Mark, A.E., Berendsen, H.J., 2005. GROMACS: fast, flexible, and free. J. Comput. Chem. 26, 1701–1718.

Wriggers, W., Chakravarty, S., Jennings, P.A., 2005. Control of protein functional dynamics by peptide linkers. Biopolymers 80, 736–746.

Yu, K., Liu, C., Kim, B.-G., Lee, D.-Y., 2015. Synthetic fusion protein design and applications. Biotechnol. Adv. 33 (1), 155–164.

Zhao, H.L., Yao, X.Q., Xue, C., Wang, Y., Xiong, X.H., Liu, Z.M., 2008. Increasing the homogeneity, stability and activity of human serum albumin and interferon-alpha2b fusion protein by linker engineering. Protein Expr. Purif. 61, 73–77.